ACS NANO

www.acsnano.org

PERSPECTIVE

Circular Polarization-Resolved Raman Optical Activity: A Perspective on Chiral Spectroscopies of Vibrational States

Engin Er,[] Tsz Him Chow,[] Luis M. Liz-Marzán,* and Nicholas A. Kotov*

Cite This: *ACS Nano* 2024, 18, 12589–12597

Read Online

ACCESS | Metrics & More | Article Recommendations

ABSTRACT: **Circular polarization-resolved Raman scattering methods include Raman optical activity (ROA) and its derivative—surface-enhanced Raman optical activity (SEROA). These spectroscopic modalities are rapidly developing due to their high information content, stand-off capabilities, and rapid development of Raman-active chiral nanostructures. These methods enable a direct readout of the vibrational energy levels of chiral molecules, crystals, and nanostructured materials, making it possible to study complex interactions and the dynamic interfaces between them. They were shown to be particularly valuable for nano- and biotechnological fields encompassing complex particles with nanoscale chirality that combine strong scattering and intense polarization rotation. This perspective dives into recent advancements in ROA and SEROA, their distinction from surface-enhanced Raman scattering, and the potential of these information-rich label-free spectroscopies for the detection of chiral biomolecules.**

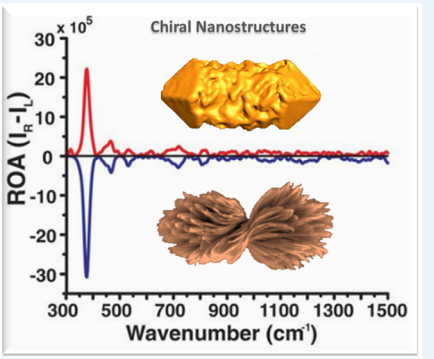

KEYWORDS: *Surface-Enhanced Raman Optical Activity, Raman Optical Activity, Surface Enhanced Raman Scattering, Chiral Phonons, Chiral Nanostructures, Label-Free*

1. CIRCULAR POLARIZATION-RESOLVED RAMAN SCATTERING: A BRIEF OVERVIEW

Chiral molecules and particles, whose mirror images cannot be superimposed onto each other, interact differently with left-handed and right-handed circularly polarized (LCP and RCP) light. Their response to light with different circular polarizations is determined by their anisotropic and complex refractive index. Differences in the imaginary part of the complex refractive index result in different absorptions of LCP and RCP light, which is known as circular dichroism (CD). On the other hand, differences in the real part of the complex refractive index induce rotation of linearly polarized light, a phenomenon known as optical rotatory dispersion (ORD). Because of the high relevance of molecular chirality in biology and medicine, it is important to develop highly sensitive techniques for the detection of molecular chirality, typically relying on CD and ORD spectroscopies. However, the chiroptical response of most biomolecules is weak (10^{-6} to 10^{-2} of absorbance differences in response to LCP and RCP light),[1] which restricts their application to sensing of chiral analytes at the microgram level. The CD and ORD response can be dramatically enhanced by nanoscale assemblies of plasmonic and semiconductor nanoparticles (NPs), due to their dimensional match with photons in the visible range of the spectrum and the high polarizability of inorganic nanostructures,[2] but the information content from these spectra is limited to the electronic excitation levels of the nanomaterials. Vibronic levels characteristic of various oscillations in the chemical structures are more informative, enabling the identification of angstrom-, nanometer-, and micrometer-scale chirality.

CD and ORD spectroscopies operate primarily in the visible and near-infrared regions, focusing on electronic transitions. Circularly polarized luminescence (CPL) from chiral nanostructures encompasses circularly polarized fluorescence and scattering, resulting from the photoexcitation of electronic states. Chiroptical spectroscopies developed for wavelengths in the mid-infrared and terahertz (THz) regions focus on vibrational energy levels and some virtual electronic states. These spectroscopies include Raman optical activity (ROA),

Received: December 31, 2023
Revised: March 20, 2024
Accepted: April 16, 2024
Published: May 6, 2024

https://doi.org/10.1021/acsnano.3c13228
ACS Nano 2024, 18, 12589–12597

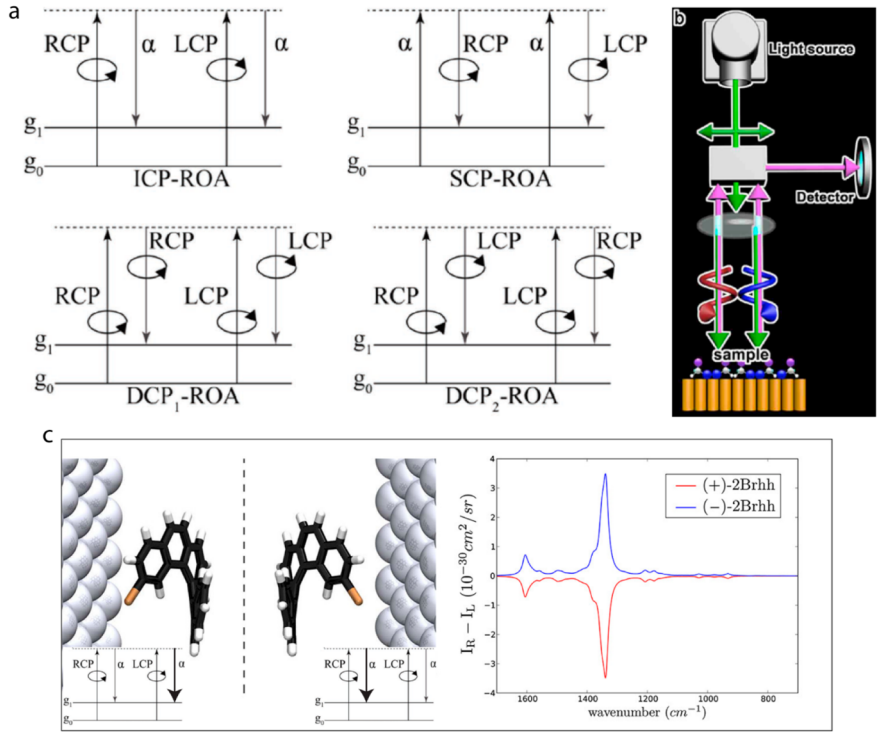

Figure 1. (a) Energy-level diagrams of different ROA measurements illustrating the definition of ROA for a molecule undergoing a transition from the zeroth (g_0) to the first (g_1) vibrational level of the ground electronic state. Reprinted with permission under a Creative Commons CC BY License from ref 15. Copyright 2018, Wiley-VCH. (b) Schematic illustration of ICP-SEROA, in which the chiral response originates from a selective interaction between chiral molecules and incident left- and right-circularly polarized light on a nanostructured plasmonic surface. Reproduced with permission from ref 10; copyright 2020, Wiley-VCH. (c) SEROA for the two enantiomers of 2Brhh on a silver surface, calculated using the dressed-tensors formalism. Insets show the energy levels involved in the Raman active vibrational modes. Reproduced with permission from ref 30; copyright 2014, American Chemical Society.

vibrational circular dichroism (VCD), and terahertz circular dichroism (TCD).[3] ROA[4] and its spectroscopic cousin known as surface-enhanced Raman optical activity (SEROA)[5] have the potential to drastically broaden the spectrum of applications of chiral spectroscopies. Starting from the pioneering works of L. Barron,[6,7] ROA has been recognized as a powerful tool to examine the structural and conformational aspects of chiral molecules, by measuring the difference of Raman scattering intensities of chiral molecules under RCP and LCP incident light. The intensity of ROA peaks depends on the chirality of the scattering molecules/particles and the polarization state of incident light relative to the molecular geometry,[3] as well as the instrument geometry, because the ROA and SEROA spectra can change drastically for side-, front-, and backscattering.[1,4] For some substrates with anisotropic placement of chiral nanostructures and Raman-active molecules/particles, the angular dependences should be taken into account as well. Under standardized conditions, by comparison of the peak positions and intensities with conventional Raman, VCD, and Fourier transform infrared (FTIR) spectroscopies, ROA adds sensitivity to mirror asymmetric oscillations. Capitalizing on information content from handedness of vibrational motions, SEROA leverages surface enhancement in high-magnitude electromagnetic fields, resulting in an amplification of weak ROA signals by several orders of magnitude and making it particularly attractive for the selective detection of enantiomers of small molecules. SEROA intensity and polarization asymmetry factor, g_{SEROA}, are commonly used parameters to quantify the degree of enantioselectivity: SEROA = $I_{RCP} - I_{LCP}$; $g_{SEROA} = 2(I_{RCP} - I_{LCP})/(I_{RCP} + I_{LCP})$,[5] where I_{LCP} and I_{RCP} are intensities of Raman scattering of LCP and RCP light.[3] The ROA spectra enhanced by chiral metamaterials have previously been utilized to discriminate between globular proteins with high α-helical content and more structurally anisotropic proteins with high β-sheet content as well as higher-order hierarchical protein structures.[8,9] Recently, the strong local chiral electromagnetic fields generated from highly polarizable chiral nanostructures, such as NPs and their assemblies, have been employed for enantiomeric discrimination by surface-enhanced Raman scattering (SERS)-chiral anisotropy effect.[10−12] High local electromagnetic field strength in assemblies of chiral/achiral plasmonic nanostructures leads to Raman scattering enhancement for both enantiomers, but one of them shows much stronger SERS signals owing to the match with molecular chirality.

2. VIBRATIONAL SPECTROSCOPIES: FROM ROA TO SEROA

Chiroptical spectroscopy techniques, such as vibrational circular dichroism (VCD) and ROA, can be employed in combination with IR and Raman spectroscopy.[4] VCD and ROA stem from the interaction between chiral compounds and circularly polarized infrared light. Due to the reasons mentioned above, these methods, collectively referred to as vibrational optical activity (VOA), are linked to changes in the energy levels of molecular vibrations within a molecule's electronic ground state. VOA measures the differential

https://doi.org/10.1021/acsnano.3c13228
ACS Nano 2024, 18, 12589−12597

response of a medium to LCP and RCP light at wavelengths corresponding to vibrational transitions in the infrared region. The VCD effect is based on different vibrational absorptions for LCP and RCP electromagnetic waves. Although it is possible to use polarized IR light to measure both the VCD and ROA effects, it is often more practical to make use of ROA, defined as the difference in Raman scattering for the RCP and LCP light. ROA is more localized and more reflective of molecular configuration, compared to VCD.[4]

ROA differs from regular Raman spectroscopy in that it provides an additional dimension of information: the sign of the spectral features, depending on whether I_{LCP} or I_{RCP} is larger. Water is an excellent solvent for Raman spectroscopy, unlike FTIR and VCD, due to the low background scattering, absorption, and luminescence. ROA spectra are more complex but offer a wealth of information. The wavenumbers of Raman and ROA bands are similar. ROA spectra are divided into four regions: low wavenumber (250−600 cm^{-1}), anomeric (600−950 cm^{-1}), fingerprint (950−1200 cm^{-1}), and CH_2/COH deformations (1200−1500 cm^{-1}).[13,14] Multiple spectral bands in ROA have been utilized to establish correlations with the secondary structures of (bio)molecules. Indeed, valuable insights have been obtained into the absolute configuration, anomeric preference, and conformation of carbohydrates. The key information that can be extracted from ROA signatures includes the absolute configuration of the anomeric center, the anomeric preference, and the orientation of the anomeric hydroxyl group, available by analysis in the low-wavenumber region and in the anomeric region.

For ROA measurements, the Stokes calculus is applied to analyze the light-scattering process. Four types of ROA measurements are commonly distinguished: (1) incident circular polarization (ICP) ROA; (2) scattered circular polarization (SCP) ROA; (3) in-phase dual circular polarization (DCP_1) ROA; (4) out-of-phase dual circular polarization (DCP_2) ROA (Figure 1a).[15] Most experimental groups use backscattering SCP-ROA, which can be accomplished using commercial Raman spectrometers, owing to a better signal-to-noise ratio. The backscattering mechanism has been developed for more than ten years. However, ROA signals are weak, 3−5 orders of magnitude weaker than the corresponding Raman scattering, which is not an example of a highly efficient spectroscopic process either. ROA is conventionally characterized by $I^R - I^L$, where I^R and I^L are the scattered intensities in right- and left-circularly polarized incident light. However, VCD utilizes the convention of subtracting right-handed from left-handed polarized light. The relative "strength" of ROA can be assessed by circular intensity difference (CID) defined as $\Delta = (I^R - I^L)/(I^R + I^L)$. The values of CID for ROA are usually less than 10^{-3}.

ROA requires long acquisition times and is associated with strong background noise, which hinders both the selectivity and the sensitivity of chiral analysis. Therefore, enhancement of the ROA is needed to accurately determine the vibrational fingerprints of molecules and NPs. Similar to SERS, SEROA can be achieved through the enhancement provided (mainly) by the high electric fields induced when plasmon resonances are excited in metal nanostructures.[16,17] The collective oscillations of free charge carriers in plasmonic systems lead to the concentration of light into near-field regions at the nanoscale, thereby providing an efficient way for the manipulation of light intensity, propagation direction, and polarization at nanoscale.[18] The large electromagnetic field at "hotspots" has been reported to enhance the Raman scattering signal of nearby molecules by as much as 10^8 times, enabling extremely high sensitivity, even down to single molecule detection under certain conditions,[19] as well as selectivity of specific vibrational signals in complex matrices.[20]

As early as 1983, Efrima successfully demonstrated the possibility to combine plasmonic enhancement with ROA, to achieve SEROA for chiral molecules adsorbed onto a metal surface.[21] The concept of incident circular polarization-SEROA (ICP-SEROA) is schematically illustrated in Figure 1b, where the chiral response stems from the specific interaction between chiral materials and incident circularly polarized light on SERS substrates. Kenipp et al. used the DCP_1 ROA setup to record CID signals of adenine in silver colloidal solution, 1 order of magnitude higher than the best values reported for classical ROA.[22] At 10 μg/mL adenine in silver colloidal solution, a 50 mW excitation laser yielded a SEROA spectrum in 10 s, whereas classic ROA demands at least 10 mg/mL, several hours of collection time, and 700−1000 mW lasers.

SERS alone has additionally been explored as a method for identifying chiral molecules without relying on the signal differences under LCP and RCP light excitation. However, this approach often necessitates the modification of SERS substrates by using chiral selectors or homochiral environments. Such modifications might potentially impact the chiral sensing process or compromise sensitivity and selectivity in chiral discrimination.[23−27] Similar to SERS, harnessing plasmonic hotspots is one of the most promising strategies for boosting the peak intensity. However, it should also be noted that plasmonic hotspots utilized in SEROA do not necessarily mean chiral hotspots because the chirality of metal NP substrates depends on collective mirror asymmetric plasmon modes, formed along the entire structure.[28,29] For example, a dimer of nanorods is chiral when they are tilted with respect to each other but cannot possess chiral character for configurations where both dipoles are exactly parallel to each other, resulting in a zero net dipole moment. Plasmonic NP-based substrates possessing both plasmonic and chiral hotspots should be fabricated under tight control of the collective plasmon modes. Based on atomistic electrodynamics−quantum mechanical models simulating SEROA for the two enantiomers of 2-bromohexahelicene, SEROA intensity could be maximized by manipulating the local electric field and field gradient, the orientation of the molecule, and the surface plasmon frequency width (Figure 1c).[30]

Chiral plasmonic metal nanostructures have recently demonstrated chiral electromagnetic field enhancement and strong interaction with chiral materials,[8,31] which is highly beneficial in SEROA. Moreover, the local asymmetric sites (chiral component) exposed on chiral NPs induce stereospecific molecular interactions, enabling direct label-free chiral differentiation.[10−12] The so-called superchiral fields (i.e., those whose chiral dissymmetry exceeds that of the fully circularly polarized light) generated by chiral Shuriken metamaterials (Figure 2a) have been utilized to discriminate between globular proteins with high α-helical content and more structurally anisotropic proteins with high β-sheet content.[9] The strong local chiral electromagnetic field generated by highly polarizable chiral platforms (*i.e.*, chiral nanostructured Au films and chiral triangular nanorings, Figure 2b,c) have been employed for enantiomeric discrimination by chiral anisotropy of SERS, induced by the chiral-selective enhance-

https://doi.org/10.1021/acsnano.3c13228
ACS Nano 2024, 18, 12589−12597

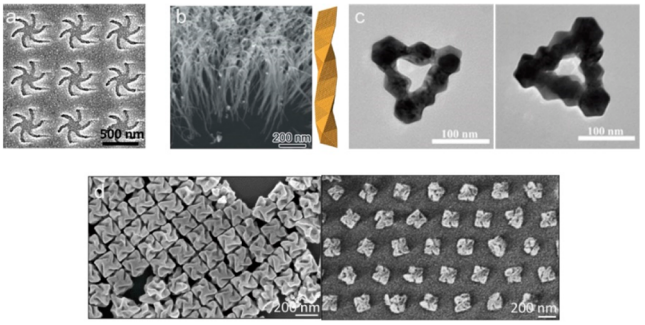

Figure 2. (a) Scanning electron microscope images of a left-handed templated plasmonic substrate. Reproduced with permission from ref 9; copyright 2015, American Chemical Society. (b) SEM image (left) of helical Au nanofibers vertically grown on a Si wafer and the corresponding scheme (right) of a right-handed chiral Au fiber. Reproduced with permission from ref 10; copyright 2020, Wiley-VCH. (c) TEM images of *L*-Pt@Au (left) and *D*-Pt@Au (right) triangular nanorings. Reproduced with permission from ref 11; copyright 2021, Wiley-VCH (d) SEM images of helicoids before (left) and after templated assembly (right). Reproduced with permission from ref 12; Copyright 2022, Nature Publishing Group.

ment between enantiomers.[10,11] A biomolecular sensor platform has been more recently realized by 432 helicoid III NPs (helicoids) to detect microRNA-21 (miR-21) and the soluble *N*-ethylmaleimide-sensitive factor attachment protein receptor (SNARE) complex (Figure 2d). The miR-21 sensor was located on the helicoids, while the SNARE segment was positioned between the helicoids.

3. CHIRAL PHONONS: LONG-RANGE VIBRATIONAL STATES WITH A TWIST

Besides local vibrational states typical for the small molecules described above, ROA and SEROA can detect the long-range coherent vibrations of multiple coupled bonds. They typically propagate through the crystal structure but can also be standing waves, commonly referred to as phonons. When these long-range oscillations have concerted twisting or rotational motion, they are called *chiral phonons*. Chirality of phonons manifests itself as vibrational patterns within solids, where the constituent atoms exhibit perpendicular rotational movement relative to their propagation direction. Chiral crystals and nanostructures, both organic and inorganic, lift degeneracy for left-handed and right-handed phonons, resulting in strong circular polarization-resolved vibrational spectra. The asymmetry of molecular geometries and related rotations in chiral nanostructures can be inferred from the intensity and spectral position of chiral phonons, which makes ROA/SEROA particularly important.[32]

The collective transversal and longitudinal motions of atoms in chiral phonons lead to circular polarization and nonzero angular momentum. Chiral phonons possess, therefore, strong orbital magnetic moments, leading to a phonomagnetic effect akin to the optomagnetic effect observed in atomic rotations with helical structures.[33] These atomic motions have been classified based on their shape of band structures including pseudomomentum (PM) and pseudoangular momentum (PAM), which are caused from translation and rotation symmetries.[34,35] Interestingly, crystal structures present different PM and PAM behaviors that correspond to the linear and circular motions of a molecule in space. Ishito et al. developed a method to assign ROA features detected in chiral tellurium single crystals by evaluating PAM values of phonons.[36]

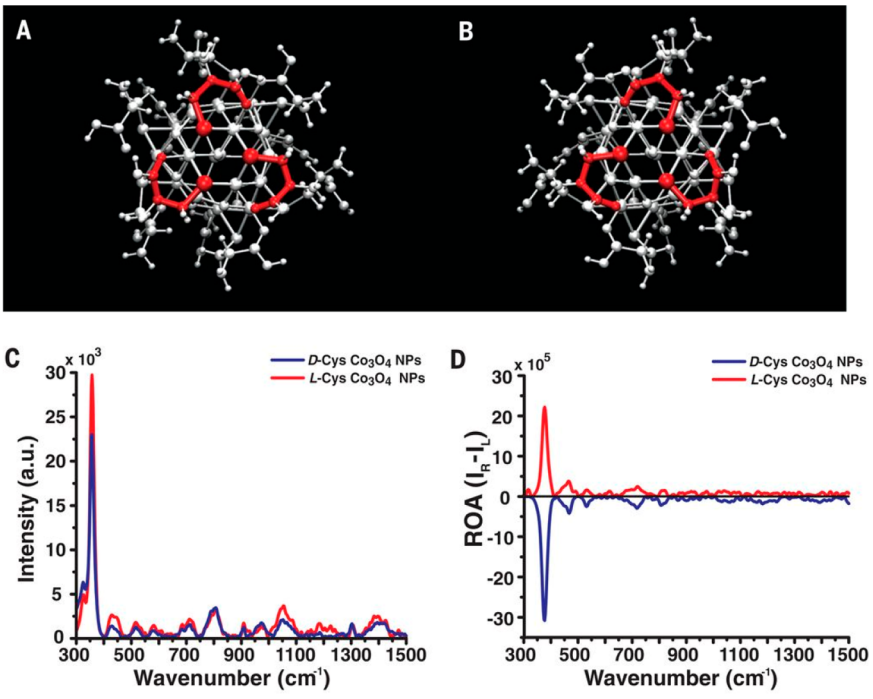

Figure 3. Schematic representation of crystalline chiral Co_3O_4 NPs, synthesized in the presence of *D*-Cys (A) and *L*-Cys (B). (C, D) Raman and ROA spectra of *D*-Cys and *L*-Cys Co_3O_4 NPs in scattered circular polarization ROA mode under 532 nm laser irradiation. Reproduced with permission from ref 37; copyright 2018, AAAS.

https://doi.org/10.1021/acsnano.3c13228
ACS Nano 2024, 18, 12589−12597

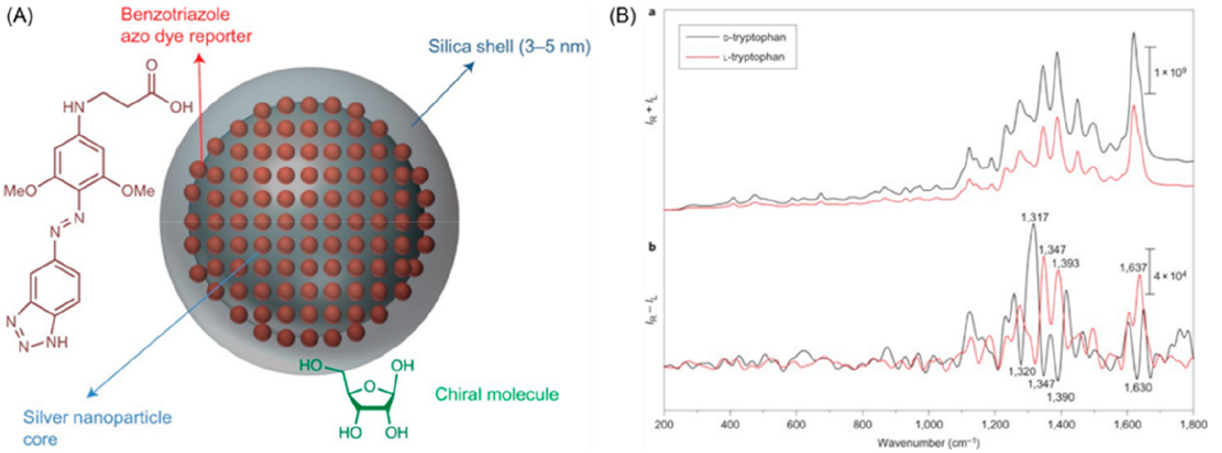

Figure 4. (A) Schematic representation of silica-coated silver nanotags as SEROA substrates. (B) SERS (upper panel) and SEROA (bottom panel) spectra of resonant *D*- and *L*-tryptophan molecules attached to silica-coated silver nanotags. Reproduced with permission from ref 50. Copyright 2015, Nature Publishing Group.

The implementation of ROA with phonon modes enables the determination of chiral distortions in the crystal lattices. For instance, Yeom et al. reported a strong chiroptical activity at 377 cm^{-1} for *D*-/*L*-cysteine (Cys)-stabilized Co_3O_4, corresponding to chiral phonons in Co_3O_4 (Figure 3).[37] Variable chiral geometries enable microstructures in specific shapes, *e.g.*, the hierarchical assembly of helical chains of Cys interconnected with Cd^{2+} ions lead to size-controlled left- and right-twisted bowties.[38] The chiroptical activity of these bowties was remarkably improved, with 10 times enhancement of chiral phonon responses in ROA.

Chiral phonons were theoretically predicted[39] and experimentally observed in transition-metal dichalcogenides (TMD), such as MoS_2, and their twisted stacks.[40,41] Ishito and co-workers reported the use of circularly polarized Raman spectroscopy to determine the chirality and ROA of three-dimensional α-HgS, by measuring the phonon mode response and splitting.[42] These results revealed the importance of phonons in the spatial imaging of chiral domains in 2D nanostructures. On the other hand, Lacinska et al. studied the chiral properties of tantalum disulfide in the 1T phase (1T-TaS_2) by polarization-resolved Raman spectroscopy. The observed phonon spectra at low-frequency regions under 532 nm laser excitation, originating from its phase transition, supported the ROA of chiral 1T-TaS_2.[43] The unusually high intensity and structural sensitivity of chiral phonons to details in a crystal lattice make a great contribution to studying the chirality of complex opaque materials on a macroscopic scale by using ROA.

4. BIOLOGICAL APPLICATIONS

Circular polarization-resolved detection of multiple vibrational levels is a spectroscopic tool with particular interest for biology. The development of SEROA was particularly useful in this respect because ROA suffers from weak and reproducible responses toward target molecules.[44] Although SEROA-based systems still suffer from problematic issues in the generation of reliable and high signal-to-noise (S/N) ratio spectra, they unexpectedly present the capability for enantiomeric separation with promising sensitivity for biomolecules. Osinska et al. successfully obtained strong SEROA signals for *D*/*L*-Cys discrimination on macroscopic rough silver substrates prepared by electrochemical techniques. Whereas the ROA spectra of *D*/*L*-Cys can be seen at high concentrations, macroscopic silver particles play a key role to generate SEROA spectra, with enhancements of 3−4 orders of magnitude compared to ROA, due to their unique structural and plasmonic properties.[45] Most often, plasmonic structures for SEROA applications involve colloidal systems, which are highly sensitive to the synthetic conditions, potentially leading to aggregation, in turn affecting the SEROA performance. Pour et al. reported the use of citrate-reduced silver colloids in the presence of polycarbopol as a stabilizing agent for *D*/*L*-ribose separation. The addition of the polymer provided a reproducible and strong SEROA signal, by reducing the effect of plasmon resonance-induced changes in circularly polarized light that typically plague SEROA experiments.[46] This example points out the high relevance of NP surface chemistry for the enhancement of analyte−plasmonic surface interactions. In an interesting piece, Das reported the self-assembly of linkers leading to spontaneous chiral aggregation on silver colloids and their subsequent use as SEROA substrates for sensing of chiral amino acids and their conformations. Specifically, mercaptopyridine derivatives were functionalized on silver surfaces to induce chirality. The results underlined the importance of linker selection on the detection of chiral molecules by SEROA. This method also allowed the detection of chiral amino acids in low concentrations, below 10^{-5} M, which represents a satisfactory sensitivity for amino acids in concentrations found in biological samples such as blood.[47]

Practical applications of SEROA are particularly relevant in the fields of protein, peptide, and DNA detection. The enhanced sensitivity offered by SEROA allows for the detection of proteins at low concentrations, including those in complex biological media. The ability to gain chiral information from these systems can advance our understanding of protein interactions and folding and misfolding, which are central to many biological processes and diseases. In this respect, we can mention the work by Johannessen et al. for the SEROA-based sensing of cytochrome c (Cytc) using colloidal silver particles. A distinct SEROA spectral pattern caused by skeletal porphyrin vibrations for Cytc was observed at concentrations as low as 1 μM, confirming the higher SEROA sensitivity toward specific vibrations that cannot be

https://doi.org/10.1021/acsnano.3c13228
ACS Nano 2024, 18, 12589−12597

detected with SERS under the same experimental conditions. The proposed SEROA substrate can be useful not only for sensing of proteins but also to learn about protein interactions in biological matrices.[48] The authors also reported the SEROA analysis of myoglobin, a protein essentially located in muscles, at the single molecule level using similar silver colloids. The resonance ROA spectra of myoglobin were remarkably improved when adsorbed on silver colloids and using a 532 nm laser. Intense and sharp chiral signals measured at the frequency range of 1300−1400 cm^{-1} in the SEROA spectrum of myoglobin, which were assigned to vibrations of haem precursor groups in its structure, confirm the efficiency of silver NPs on SEROA-based protein detection.[49]

However, plasmonic nanostructures may not have sufficiently strong chiral sensitivity to allow ROA sensing for complex biological media. For this reason, indirect sensing/binding mechanisms have been proposed, similar to the use of nanotags in immunoassays. Pour et al. reported the chiroptical behavior induced in silica-coated silver nanotags modified with achiral linker molecules (Figure 4). The enantiomeric analytes ribose and tryptophan were successfully detected on Ag@SiO_2 NPs functionalized with benzotriazoles as the plasmonic substrates for ROA enhancement. The obtained mirror-image SEROA spectra can be explained because chiral molecules attached to the silica-coated silver nanotags possess the enantioselectivity required to break the symmetric environment of the achiral plasmonic cluster. Extension of current nanotag designs will enable enhancement of chiroptical scattering peaks and better understanding of protein−ligand binding mechanisms.[50]

Sun et al. reported plasmon-enhanced ROA when surface plasmons are launched along chiral Ag nanowires. It was observed that the coupling angle and distance between Ag nanowires as well as their edge morphologies were highly sensitive toward creating surface plasmons and consequently affected the SEROA response. The ROA signal of the essential chiral peptide FMOC-glycyl-glycine−OH at 1593 cm^{-1} was significantly enhanced when chiral Ag nanowires were excited by left- and right-circularly polarized light. This unusual SEROA approach has promising potential to determine interaction mechanisms and sensing applications in biological samples.[51] The experimental approach taking advantage of the remotely excited ROA enhanced by plasmons of chiral Ag nanowires has been further addressed for the detection of adenine, which is regarded as a prochiral molecule. Similarly, Kneipp et al. developed a SEROA strategy using silver colloidal NPs (10−50 nm) for sensing of adenine. Once adenine is adsorbed on a metal surface, this nucleotide loses mirror-plane symmetry and becomes chiral. Starting from this point of view, the SEROA peaks at ∼730 cm^{-1} and ∼1330 cm^{-1}, which are assigned to ring-breathing and ring-stretching/CH-bending, respectively, indicated the successful adsorption of adenine with one preferred chiral direction on silver NPs. The proposed rapid and sensitive SEROA system, compared to classical ROA, shows potential applicability for characterization and sensing of basic biologically active molecules or racemic drugs, which have the ability of self-assembling on surfaces.[22]

5. ROA, SEROA, AND SERS: UNDERSTANDING THE DIFFERENCES

The 50th anniversary of the discovery of SERS[52−55] is an opportune moment to distinguish it from ROA and SEROA. SERS exploits the interaction between electromagnetic fields and nanoscale rough surfaces to enhance Raman signals. Although SERS, ROA, and SEROA are related techniques, they offer unique advantages. ROA and SEROA provide chiral information, with SEROA being capable of achieving a significantly enhanced sensitivity, whereas SERS offers higher sensitivity but (typically) does not provide chiral specificity. Table 1 summarizes the characteristic features of ROA, SEROA, and SERS.

6. FUTURE PERSPECTIVES & CONCLUSIONS

Chiroptical spectroscopy is a powerful tool, not only for identifying the configuration of chiral molecules and selective sensing of biomolecules in native aqueous complex media. The primary bottleneck of SEROA is obtaining strong and reproducible ROA signals. Researchers have made enormous efforts to deal with these issues by fabricating SEROA platforms based on metallic nanostructures with various shapes and sizes for chiral molecule detection. Indeed, chiral nanostructures with extraordinary chemical and optical properties offer a flexible design for SEROA-based platforms. A wide variety of substrates with variable patterns, nanoscale architecture, and hotspot chirality morphology can be obtained by means of modern nanofabrication techniques. We foresee that tailoring chiral geometry, including recently developed colloidal growth methods,[56−58] will be a key point for the future of chiral molecule separation, sensing, and interaction studies in biological applications. The observation of ROA from chiral phonons represents crucial developments in this field because of: (i) sharp and strong peak resonances; (ii) a wide range of nanostructures capable of sustaining chiral phonons, and (iii) their strong dependence on minute alterations of crystal lattices. The latter is particularly valuable for the identification of minute alterations of chiral crystal lattices. The use of chiral phonon modes may enable the implementation of a wide range of materials, such as 2D nanostructures and semiconductor hierarchical structures, as SEROA substrates with enhanced chiroptical activity.

The complex and stochastic (albeit nonrandom) orientation of target molecules on metal surfaces, including those with weak interactions, inevitably affects the chiroptical responses. Improved theoretical models are thus required to better understand the SEROA mechanisms regarding the molecular orientation to the optical surface. Optimizations including the selection of chiroptical nanostructures and experimental parameters, as well as theoretical models, may be highly informative for the future design of SEROA-based applications. It should be noted that postmodification strategies such as covalent attachment, overgrowth of metallic structures, or the use of stabilizing agents may also enhance surface−analyte interactions and consequently SEROA sensitivity. Chiral molecules that can link plasmonic NPs upon assembly can also offer advantages toward chiral molecule detection by improving surface−analyte interactions due to increased potential conformational matches. We expect that 3D chiroptical assemblies based on metallic or semiconductor NPs as scaffolds will play an important role in the progress of SEROA-based biological applications, *e.g.*, by implementing DNA origami technology for single biomolecule detection.

Considering biological, biomedical, and other applications of ROA and SEROA, one must be mindful of potential sources of artifacts. Similarly to CD, circularly polarized chiroptical bands can also be generated by achiral compounds. C.R. Lightner et al. developed an efficient Mueller-matrix model to differentiate

https://doi.org/10.1021/acsnano.3c13228
ACS Nano 2024, 18, 12589−12597

Table 1. Comparison of Characteristic Features for ROA, SEROA, and SERS

	ROA	SEROA	SERS
Principle of the technique	Differential Raman scattering of circularly polarized light by chiral molecules.	Combining the chiral sensitivity of ROA with the SERS effect.	Enhanced Raman scattering signal resulting from the LSPR of metal nanostructures.
Instrumentation	Raman spectrometer, circularly polarized light source, and optical activity detection module. Configuration: ICP-ROA, SCP-ROA, DCP_1-ROA, & DCP_2-ROA	Raman spectrometer, circularly polarized light source, optical activity detection module, and SERS substrate.	SERS substrate, Raman spectrometer, laser source, and IR detector.
Enantiomer differentiation	ROA is specifically designed to differentiate between enantiomers.	SEROA allows for sensitive sensing of chiral molecules at low concentrations while preserving the enantiomer differentiation capability.	Additional strategies must be employed, such as chiral plasmonic platforms, chiral auxiliary molecules, or chiral recognition agents.
Signal strength	No signal enhancement, CID typically ~10^{-3}	Moderate signal enhancement, CID ≥ 10^{-3}	Strong enhancement, up to 10^8
Applications	Determination of absolute configuration, conformational analysis, and study of molecular interactions.	Sensitive analysis of chiral molecules at low concentrations in biochemical and pharmaceutical applications, and chirality recognition.	Single-molecule detection ability in biosensing and biomedical applications, single-molecule detection.
Limitations	(1) Sensitivity (2) Strict requirement for molecules with sufficiently strong Raman scattering (3) Instrumental complexity	(1) Heat generation through plasmonic photothermal effects (2) Additional functionalization strategies may be necessary, such as linker molecule attachment to a metal surface (3) Limited availability of substrates and substrate reproducibility	(1) Enhancement variability and substrate homogeneity (2) Interference from background signals and signal reproducibility

ROA responses from the artifacts generated from chiral or achiral target molecules.[59] Specifically, achiral invariants can lead to linear depolarization and circular depolarization, resulting in measurable ROA signals. Based on their findings, with the elimination of these artifacts using component decomposition identical to Muller Matrix polarimetry (MMP), improvements not only in the sensitivity but also in the reproducibility of ROA signals can be made. It is particularly significant that these advances and accounting of MMP artifacts will be in ROA studies of chiral solids with strong Raman scattering. They can be exemplified by chiral perovskites and chiral carbons. Development of the substrates with variable left/right long/short pitch of plasmonic helicoids obtained by scalable light-to-matter chirality transfer[60] enables us to produce the scalable multiplexed ROA/SEROA assays that can further increase the confidence and information content of the MMP images and SEROA spectroscopic data sets.

Recent advances in synthetic techniques have enabled the preparation of chiral NPs with diverse compositions, sizes, shapes, and precisely controlled twisted surface geometries.[61] Incorporating these chiral NPs into ROA holds significant promise in enhancing the chiroptical response and eliminating some of the pervasive artifacts. This integration aims to generate chiral electromagnetic near fields on NP surfaces with robust interaction with chiral molecules. Well-defined chiral plasmonic nanostructures should also standardize the generation and optimize the geometry of the electromagnetic fields at plasmonic hotspots. These fields play a pivotal role in facilitating chiral discrimination and effectively determining biomolecular handedness. In addition to plasmonic NPs, dielectric nanomaterials offer an exciting path toward SEROA.[62] All-dielectric NPs may allow the elimination of spectral artifacts arising from photothermal heat generation, which is a potential limitation for plasmonic metal nanostructures. Furthermore, they address the inefficiency in transferring and enhancing optical chirality from the far field to the near field. Leveraging the unique attributes of chiral NPs holds promise for advancing SEROA into a robust tool capable of probing biomolecular configurations and elucidating complex biological structures at higher hierarchical levels.

AUTHOR INFORMATION

Corresponding Authors

Luis M. Liz-Marzán − *CIC biomaGUNE, Basque Research and Technology Alliance (BRTA), Donostia-San Sebastián 20014, Spain; Ikerbasque, Basque Foundation for Science, Bilbao 43009, Spain; Centro de Investigación Biomédica en Red, Bioingeniería, Biomateriales y Nanomedicina (CIBER-BBN), Donostia-San Sebastián 20014, Spain; Cinbio, University of Vigo, Vigo 36310, Spain;* orcid.org/0000-0002-6647-1353; Email: llizmarzan@cicbiomagune.es

Nicholas A. Kotov − *Department of Chemical Engineering, Department of Materials Science, and Biointerfaces Institute, University of Michigan, Ann Arbor 48109-2102 Michigan, United States; NSF Center for Complex Particle Systems (COMPASS), Ann Arbor 48109 Michigan, United States;* orcid.org/0000-0002-6864-5804; Email: kotov@umich.edu

Authors

Engin Er − *Department of Chemical Engineering, University of Michigan, Ann Arbor 48109-2102 Michigan, United States;*

https://doi.org/10.1021/acsnano.3c13228
ACS Nano 2024, 18, 12589−12597

NSF Center for Complex Particle Systems (COMPASS), Ann Arbor 48109 Michigan, United States; Biotechnology Institute, Ankara University, Ankara 06135, Turkey

Tsz Him Chow − *CIC biomaGUNE, Basque Research and Technology Alliance (BRTA), Donostia-San Sebastián 20014, Spain*

Complete contact information is available at: https://pubs.acs.org/10.1021/acsnano.3c13228

Author Contributions

◨(E.E. and T.H.C.) These authors have contributed equally to this work.

Notes

The authors declare no competing financial interest.

ACKNOWLEDGMENTS

T.H.C. and L.M.L.-M. acknowledge funding from the European Commission, under grant HORIZON-TMA-MSCA-PF-EF, SEP-210883629 (ChirPlasBiosensing). N.A.K. and E.E. acknowledge funding from the National Science Foundation NSF 2243104. "Center of Complex Particle Systems (COMPASS)"; Office of Naval Research Vannevar Bush DoD Fellowship "Engineered Chiral Ceramics"; and ONR N000141812876 and MURI project "Mechanics or Metamaterials" ONR N00014-20-1-2479. E.E. acknowledges a grant by U.S. Fulbright Visiting Scholar Program, which is sponsored by the U.S. Department of State and Turkish Fulbright Commission. E.E. thanks Ankara University Scientific Research Projects Coordination Unit for financial support under grant TSA-2023-2751.

REFERENCES

(1) Tang, Y.; Cohen, A. E. Optical Chirality and Its Interaction with Matter. *Phys. Rev. Lett.* **2010**, *104*, 163901.

(2) Chen, W.; Bian, A.; Agarwal, A.; Liu, L.; Shen, H.; Wang, L.; Xu, C.; Kotov, N. A. Nanoparticle Superstructures Made by Polymerase Chain Reaction: Collective Interactions of Nanoparticles and a New Principle for Chiral Materials. *Nano Lett.* **2009**, *9*, 2153−2159.

(3) Choi, W. J.; Cheng, G.; Huang, Z.; Zhang, S.; Norris, T. B.; Kotov, N. A. Terahertz Circular Dichroism Spectroscopy of Biomaterials Enabled by Kirigami Polarization Modulators. *Nat. Mater.* **2019**, *18*, 820−826.

(4) Nafie, L. A. Vibrational optical activity: From discovery and development to future challenges. *Chirality* **2020**, *32* (5), 667−692.

(5) Abdali, S.; Blanch, E. W. Surface enhanced Raman optical activity (SEROA). *Chem. Soc. Rev.* **2008**, *37*, 980−992.

(6) Barron, L. D.; Buckingham, A. D. Rayleigh and Raman Scattering from Optically Active Molecules. *Mol. Phys.* **1971**, *20*, 1111−1119.

(7) Barron, L. D. *Molecular Light Scattering and Optical Activity*, 2nd ed.; Cambridge University Press: Cambridge, UK, 2004.

(8) Hendry, E.; Carpy, T.; Johnston, J.; Popland, M.; Mikhaylovskiy, R. V.; Lapthorn, A. J.; Kelly, S. M.; Barron, L. D.; Gadegaard, N.; Kadodwala, M. Ultrasensitive Detection and Characterization of Biomolecules Using Superchiral Fields. *Nat. Nanotechnol.* **2010**, *5*, 783−787.

(9) Tullius, R.; Karimullah, A. S.; Rodier, M.; Fitzpatrick, B.; Gadegaard, N.; Barron, L. D.; Rotello, V. M.; Cooke, G.; Lapthorn, A.; Kadodwala, M. Superchiral" Spectroscopy: Detection of Protein Higher Order Hierarchical Structure with Chiral Plasmonic Nanostructures. *J. Am. Chem. Soc.* **2015**, *137*, 8380−8383.

(10) Liu, Z.; Ai, J.; Kumar, P.; You, E.; Zhou, X.; Liu, X.; Tian, Z.; Bouř, P.; Duan, Y.; Han, L.; Kotov, N. A.; Ding, S.; Che, S. Enantiomeric Discrimination by Surface-Enhanced Raman Scattering − Chiral Anisotropy of Chiral Nanostructured Gold Films. *Angew. Chem., Int. Ed.* **2020**, *59*, 15226−15231.

(11) Wang, G.; Hao, C.; Ma, W.; Qu, A.; Chen, C.; Xu, J.; Xu, C.; Kuang, H.; Xu, L. Chiral Plasmonic Triangular Nanorings with SERS Activity for Ultrasensitive Detection of Amyloid Proteins in Alzheimer's Disease. *Adv. Mater.* **2021**, *33*, 2102337.

(12) Kim, R. M.; Huh, J.-H.; Yoo, S.; Kim, T. G.; Kim, C.; Kim, H.; Han, J. H.; Cho, N. H.; Lim, Y.-C.; Im, S. W.; et al. Enantioselective Sensing by Collective Circular Dichroism. *Nature* **2022**, *612*, 470−476.

(13) Wen, Z. Q.; Barron, L. D.; Hecht, L. Vibrational Raman Optical Activity of Monosaccharides. *J. Am. Chem. Soc.* **1993**, *115*, 285−292.

(14) Dudek, M.; Zajac, G.; Szafraniec, E.; Wiercigroch, E.; Tott, S.; Malek, K.; Kaczor, A.; Baranska, M. Raman Optical Activity and Raman Spectroscopy of Carbohydrates in Solution. *Spectrochim. Acta, Part A* **2019**, *206*, 597−612.

(15) Collins, J. T.; Kuppe, C.; Hooper, D. C.; Sibilia, C.; Centini, M.; Valev, V. K. Chirality and Chiroptical Effects in Metal Nanostructures: Fundamentals and Current Trends. *Adv. Optical Mater.* **2017**, *5*, 1700182.

(16) Olson, J.; Dominguez-Medina, S.; Hoggard, A.; Wang, L.-Y.; Chang, W.-S.; Link, S. Optical Characterization of Single Plasmonic Nanoparticles. *Chem. Soc. Rev.* **2015**, *44*, 40−57.

(17) Langer, J.; Jimenez de Aberasturi, D.; Aizpurua, J.; Alvarez-Puebla, R. A.; Auguié, B.; Baumberg, J. J.; Bazan, G. C.; Bell, S. B. J.; Boisen, A.; Brolo, A. G.; et al. Present and Future of Surface-Enhanced Raman Scattering. *ACS Nano* **2020**, *14*, 28−117.

(18) Liz-Marzán, L. M.; Murphy, C. J.; Wang, J. Nanoplasmonics. *Chem. Soc. Rev.* **2014**, *43*, 3820−3822.

(19) Nie, S.; Emory, S. R. Probing Single Molecules and Single Nanoparticles by Surface-Enhanced Raman Scattering. *Science* **1997**, *275*, 1102−1106.

(20) Plou, J.; Valera, P. S.; García, I.; de Albuquerque, C. D. L.; Carracedo, A.; Liz-Marzán, L. M. Prospects of Surface-Enhanced Raman Spectroscopy for Biomarker Monitoring toward Precision Medicine. *ACS Photonics* **2022**, *9*, 333−350.

(21) Efrima, S. The effect of large electric field gradients on the Raman Optical Activity of Molecules Adsorbed on Metal Surfaces. *Chem. Phys. Lett.* **1983**, *102*, 79−82.

(22) Kneipp, H.; Kneipp, J.; Kneipp, K. Surface-Enhanced Raman Optical Activity on Adenine in Silver Colloidal Solution. *Anal. Chem.* **2006**, *78*, 1363−1366.

(23) Li, H.; Zhang, J.; Jiang, L.; Yuan, R.; Yang, X. Chiral Plasmonic Au−Ag Core Shell Nanobipyramid for SERS Enantiomeric Discrimination of Biologically Relevant Small Molecules. *Anal. Chim. Acta* **2023**, *1239*, 340740.

(24) Wang, Y.; Yu, Z.; Ji, W.; Tanaka, Y.; Sui, H.; Zhao, B.; Ozaki, Y. Enantioselective Discrimination of Alcohols by Hydrogen Bonding: A SERS Study. *Angew. Chem., Int. Ed.* **2014**, *53*, 13866−13870.

(25) Xu, J.; Xue, Y.; Jian, X.; Zhao, Y.; Dai, Z.; Xu, J.; Gao, Z.; Mei, Y.; Song, Y.-Y. Understanding of Chiral Site-Dependent Enantioselective Identification on a Plasmon-Free Semiconductor Based SERS Substrate. *Chem. Sci.* **2022**, *13*, 6550−6557.

(26) Wang, Y.; Zhao, X.; Yu, Z.; Xu, Z.; Zhao, B.; Ozaki, Y. A Chiral-Label-Free SERS Strategy for the Synchronous Chiral Discrimination and Identification of Small Aromatic Molecules. *Angew. Chem., Int. Ed.* **2020**, *59*, 19079−19086.

(27) Abalde-Cela, S.; Hermida-Ramón, J. M.; Contreras-Carballada, P.; De Cola, L.; Guerrero-Martínez, A.; Alvarez-Puebla, R. A.; Liz-Marzán, L. M. SERS Chiral Recognition and Quantification of Enantiomers through Cyclodextrin Supramolecular Complexation. *ChemPhysChem* **2011**, *12*, 1529−1535.

(28) Hentschel, M.; Schaferling, M.; Duan, X.; Giessen, H.; Liu, N. Chiral Plasmonics. *Sci. Adv.* **2017**, *3*, e1602735.

(29) Auguié, B.; Alonso-Gómez, J. L.; Guerrero-Martínez, A.; Liz-Marzán, L. M. Fingers Crossed: Optical Activity of a Chiral Dimer of Plasmonic Nanorods. *J. Phys. Chem. Lett.* **2011**, *2*, 846−851.

(30) Chulhai, D. V.; Jensen, L. Simulating Surface-Enhanced Raman Optical Activity Using Atomistic Electrodynamics-Quantum Mechanical Models. *J. Phys. Chem. A* **2014**, *118*, 9069−9079.

(31) Obelleiro-Liz, M.; Martín, V. F.; Solís, D. M.; Taboada, J. M.; Obelleiro, F.; Liz-Marzán, L. M. Influence of Geometrical Parameters on the Optical Activity of Chiral Gold Nanorods. *Adv. Optical Mater.* **2023**, *11*, 2203090.
(32) Zhu, H.; Yi, J.; Li, M.-Y.; Xiao, J.; Zhang, L.; Yang, C.-W.; Kaindl, R. A.; Li, L.-J.; Wang, Y.; Zhang, X. Observation of Chiral Phonons. *Science* **2018**, *359*, 579−582.
(33) Ueda, H.; García-Fernández, M.; Agrestini, S.; Romao, C. P.; van den Brink, J.; Spaldin, N. A.; Zhou, K.-J.; Staub, U. Chiral Phonons in Quartz Probed by X-Rays. *Nature* **2023**, *618*, 946.
(34) Zhang, L.; Niu, Q. Chiral Phonons at High-Symmetry Points in Monolayer Hexagonal Lattices. *Phys. Rev. Lett.* **2015**, *115*, 115502.
(35) Chen, H.; Zhang, W.; Niu, Q.; Zhang, L. Chiral Phonons in Two-Dimensional Materials. *2D Mater.* **2019**, *6*, No. 012002.
(36) Ishito, K.; Mao, H.; Kobayashi, K.; Kousaka, Y.; Togawa, Y.; Kusunose, H.; Kishine, J.; Satoh, T. Chiral Phonons: Circularly Polarized Raman Spectroscopy and Ab Initio Calculations in a Chiral Crystal Tellurium. *Chirality* **2023**, *35*, 338−345.
(37) Yeom, J.; Santos, U. S.; Chekini, M.; Cha, M.; De Moura, A. F.; Kotov, N. A. Chiromagnetic Nanoparticles and Gels. *Science* **2018**, *359*, 309−314.
(38) Kumar, P.; Vo, T.; Cha, M.; Visheratina, A.; Kim, J.-Y.; Xu, W.; Schwartz, J.; Simon, A.; Katz, D.; Nicu, V. P.; et al. Photonically Active Bowtie Nanoassemblies with Chirality Continuum. *Nature* **2023**, *615*, 418−425.
(39) Zhang, L.; Niu, Q. Chiral Phonons at High-Symmetry Points in Monolayer Hexagonal Lattices. *Phys. Rev. Lett.* **2015**, *115*, 115502.
(40) Suri, N.; Wang, C.; Zhang, Y.; Xiao, D. Chiral Phonons in Moiré Superlattices. *Nano Lett.* **2021**, *21*, 10026−10031.
(41) Zhang, S.; Pei, Y.; Hu, S.; Wu, N.; Chen, D.-Q.; Lian, C.; Meng, S. Light-Induced Phonon-Mediated Magnetization in Monolayer MoS_2. *Chin. Phys. Lett.* **2023**, *40*, No. 077502.
(42) Ishito, K.; Mao, H.; Kousaka, Y.; Togawa, Y.; Iwasaki, S.; Zhang, T.; Murakami, S.; Kishine, J.; Satoh, T. Truly Chiral Phonons in α-HgS. *Nat. Phys.* **2023**, *19*, 35−39.
(43) Lacinska, E. M.; Furman, M.; Binder, J.; Lutsyk, I.; Kowalczyk, P. J.; Stepniewski, R.; Wysmolek, A. Raman Optical Activity of 1T-TaS_2. *Nano Lett.* **2022**, *22*, 2835−2842.
(44) Zhu, S.; Sun, M. Electronic Circular Dichroism and Raman Optical Activity: Principle and Applications. *Appl. Spectrosc. Rev.* **2021**, *56*, 553−587.
(45) Osińska, K.; Pecul, M.; Kudelski, A. Circularly Polarized Component in Surface-Enhanced Raman Spectra. *Chem. Phys. Lett.* **2010**, *496*, 86−90.
(46) Pour, S. O.; Bell, S. E. J.; Blanch, E. W. Use of a Hydrogel Polymer for Reproducible Surface Enhanced Raman Optical Activity (SEROA). *Chem. Commun.* **2011**, *47*, 4754−4756.
(47) Das, M.; Gangopadhyay, D.; Šebestík, J.; Habartová, L.; Michal, P.; Kapitán, J.; Bouř, P. Chiral Detection by Induced Surface-Enhanced Raman Optical Activity. *Chem. Commun.* **2021**, *57*, 6388−6391.
(48) Johannessen, C.; White, P. C.; Abdali, S. Resonance Raman Optical Activity and Surface Enhanced Resonance Raman Optical Activity Analysis of Cytochrome C. *J. Phys. Chem. A* **2007**, *111*, 7771−7776.
(49) Abdali, S.; Johannessen, C.; Nygaard, J.; Nørbygaard, T. Resonance Surface Enhanced Raman Optical Activity of Myoglobin as a Result of Optimized Resonance Surface Enhanced Raman Scattering Conditions. *J. Phys.: Cond. Matt.* **2007**, *19*, 285205.
(50) Ostovar pour, S.; Rocks, L.; Faulds, K.; Graham, D.; Parchansky, V.; Bour, P.; Blanch, E. W. Through-Space Transfer of Chiral Information Mediated by a Plasmonic Nanomaterial. *Nat. Chem.* **2015**, *7*, 591−596.
(51) Sun, M.; Zhang, Z.; Wang, P.; Li, Q.; Ma, F.; Xu, H. Remotely Excited Raman Optical Activity Using Chiral Plasmon Propagation in Ag Nanowires. *Light Sci. Appl.* **2013**, *2*, e112.
(52) Fleischmann, M.; Hendra, P. J.; McQuillan, A. J. Raman Spectra of Pyridine Adsorbed at a Silver Electrode. *Chem. Phys. Lett.* **1974**, *26*, 163−166.
(53) Jeanmaire, D. L.; Van Duyne, R. P. Surface Raman Spectroelectrochemistry: PartI. Aromatic, and Aliphatic Amines Adsorbed on the Anodized Silver Electrode. *J. Electroanal. Chem.* **1977**, *84*, 1−20.
(54) Albrecht, M. G.; Creighton, J. A. Anomalously Intense Raman Spectra of Pyridine at a Silver Electrode. *J. Am. Chem. Soc.* **1977**, *99*, 5215−5217.
(55) Liz-Marzán, L. M.; Willets, K. A.; Chen, X. 50 Years of Surface-Enhanced Spectroscopy. *ACS Nano* **2024**, *18*, 5995.
(56) Lee, H.-E.; Ahn, H.-Y.; Mun, J.; Lee, Y. Y.; Kim, M.; Cho, N. H.; Chang, K.; Kim, W. S.; Rho, J.; Nam, K. T. Amino-Acid- and Peptide-Directed Synthesis of Chiral Plasmonic Gold Nanoparticles. *Nature* **2018**, *556*, 360−365.
(57) González-Rubio, G.; Mosquera, J.; Kumar, V.; Pedrazo-Tardajos, A.; Llombart, P.; Solís, D. M.; Lobato, I.; Noya, E. G.; Guerrero-Martínez, A.; Taboada, J. M.; et al. Micelle-Directed Chiral Seeded Growth on Anisotropic Gold Nanocrystals. *Science* **2020**, *368*, 1472−1477.
(58) Ni, B.; Mychinko, M.; Gómez-Graña, S.; Morales-Vidal, J.; Obelleiro-Liz, M.; Heyvaert, W.; Vila-Liarte, D.; Zhuo, X.; Albrecht, W.; Zheng, G.; et al. Chiral Seeded Growth of Gold Nanorods Into Fourfold Twisted Nanoparticles with Plasmonic Optical Activity. *Adv. Mater.* **2023**, *35*, 2208299.
(59) Lightner, C. R.; Desmet, F.; Gisler, D.; Meyer, S. A.; Perez Mellor, A. F.; Niese, H.; Rosspeintner, A.; Keitel, R. C.; Bürgi, T.; Herrebout, W. A.; et al. Understanding Artifacts in Chiroptical Spectroscopy. *ACS Photonics* **2023**, *10*, 475−483.
(60) Kim, J.-Y.; et al. Direct-write 3D printing of plasmonic nanohelicoids by circularly polarized light. *Proc. Natl. Acad. Sci. U. S. A.* **2024**, *121*, 11.
(61) Cho, N. H.; Guerrero-Martínez, A.; Ma, J.; Bals, S.; Kotov, N. A.; Liz-Marzán, L. M.; Nam, K. T. Bioinspired Chiral Inorganic Nanomaterials. *Nat. Rev. Bioeng.* **2023**, *1*, 88−106.
(62) Xiao, T.-H.; Cheng, Z.; Luo, Z.; Isozaki, A.; Hiramatsu, K.; Itoh, T.; Nomura, M.; Iwamoto, S.; Goda, K. All-Dielectric Chiral-Field-Enhanced Raman Optical Activity. *Nat. Commun.* **2021**, *12*, 3062.

https://doi.org/10.1021/acsnano.3c13228
ACS Nano 2024, 18, 12589−12597